HHS Public Access

Author manuscript

Mol Microbiol. Author manuscript; available in PMC 2020 August 14.

Published in final edited form as:

Mol Microbiol. 2018 April ; 108(2): 143–158. doi:10.1111/mmi.13923.

Leishmania mexicana can utilize amino acids as major carbon sources in macrophages but not in animal models

Eleanor C. Saunders[1], **Thomas Naderer**[1], **Jenny Chambers**[1], **Scott M. Landfear**[2], **Malcolm J. McConville**[1]

[1]Department of Biochemistry and Molecular Biology, Bio21 Molecular Science and Biotechnology Institute, University of Melbourne, 30 Flemington Road, Parkville, Victoria, 3010 Australia

[2]Molecular Microbiology & Immunology, Oregon Health Sciences University, Portland, OR 97239, USA

Abstract

Leishmania parasites target macrophages in their mammalian hosts and proliferate within the mature phagolysosome compartment of these cells. Intracellular amastigote stages are dependent on sugars as a major carbon source *in vivo*, but retain the capacity to utilize other carbon sources. To investigate whether amastigotes can switch to using other carbon sources, we have screened for suppressor strains of the *L. mexicana Δlmxgt1–3* mutant which lacks the major glucose transporters LmxGT1–3. We identified a novel suppressor line (*Δlmxgt1–3*^{s2}) that has restored growth in rich culture medium and virulence in *ex vivo* infected macrophages, but failed to induce lesions in mice. *Δlmxgt1–3*^{s2} amastigotes had lower rates of glucose utilization than the parental line and primarily catabolized non-essential amino acids. The increased mitochondrial metabolism of this line was associated with elevated levels of intracellular reactive oxygen species, as well as increased sensitivity to inhibitors of the tricarboxylic acid (TCA) cycle, including nitric oxide. These results suggest that hardwired sugar addiction of *Leishmania* amastigotes contributes to the intrinsic resistance of this stage to macrophage microbicidal processes *in vivo,* and that these stages have limited capacity to switch to using other carbon sources.

Plain language summary

Leishmania parasites target macrophages and other immune cells in their animal host and reside within a nutrient-rich lysosomal compartment. Here we show that intracellular parasites are addicted to using sugars as their major carbon source as utilization of other nutrients (amino acids) leads to increased sensitivity to host anti-microbial responses. These findings indicate that resistance to drugs that target sugar metabolism will be slow to evolve.

Correspondence to: Professor Malcolm McConville, malcolmm@unimelb.edu.au, Tel: 61-3-8344 2342.

Author Contributions

ECS and MJM contributed to the conception and design of the study. ECS, JC, TN and MJM contributed to the acquisition, analysis and interpretation of the data. SML provided essential cell lines. ECS, SML and MJM contributed to the writing of the manuscript.

Introduction

Leishmania are sandfly-transmitted parasitic protists that are thought to chronically infect more than 120 million people world-wide, causing a spectrum of diseases in 12 million people ranging from self-healing cutaneous lesions to life-threatening visceral infections (Pigott *et al.*, 2014). Infection is initiated by promastigote stages which are injected into the skin during a sandfly bloodmeal, and are rapidly internalized by monocytes and macrophages, either directly or after passage through short-lived neutrophils. Unlike most other microbial pathogens that target macrophages, *Leishmania* are delivered directly to the mature phagolysosome compartment where they differentiate into a non-motile amastigote stage. Depending on the *Leishmania* species involved, amastigotes can either reside within tight-fitting, individual or large spacious communal phagolysosomes. Amastigotes can reside long term within this hydrolytic compartment and are responsible for causing both acute inflammatory infections as well as long-term chronic infections.

In contrast to most other vacuolar compartments in macrophages, the mature phagolysosome is thought to contain a variety of potential carbon sources, including sugars, amino acids and lipids generated by the constitutive degradation of internalized macromolecules, extracellular matrix and apoptotic cell debris (McConville and Naderer, 2011). However, recent studies suggest that *Leishmania* amastigotes may switch to a slow growing, metabolically quiescent state in this niche (Kloehn *et al.*, 2015; Kloehn *et al.*, 2016). This switch appears to be independent of nutrient levels and tightly linked to amastigote differentiation, and may ensure that intracellular stages do not overgrow this niche and deplete other less abundant nutrients for which they are auxotrophic, including many amino acids, purines, vitamins and heme (McConville and Naderer, 2011).

Notwithstanding the availability of different carbon sources in the macrophage phagolysosome, *Leishmania* amastigotes appear to be highly dependent on sugars as a major source *in vivo*. This is supported by metabolomic analyses which show that amastigotes preferentially catabolize glucose (or other sugars) over amino acids *in vitro* (Saunders *et al.*, 2014). While amastigotes also use fatty acids as a carbon source, carbon skeletons derived from fatty acid β-oxidation are primarily catabolized in the TCA cycle and used to synthesize non-essential amino acids (NEAA) rather than used for gluconeogenesis or energy production (Saunders *et al.*, 2014). Second, *Leishmania* amastigotes accumulate the novel carbohydrate reserve material, mannogen (β−1,2-linked mannose oligomers), suggesting that these stages may have access to a constant supply of sugars for growth and persistence in this niche (Sernee *et al.*, 2006). Finally, genetic disruption of hexose uptake or catabolism results in loss of virulence. Specifically, a *L. mexicana* mutant lacking three facilitative hexose transporters (*Δlmxgt1–3*) exhibits attenuated growth in culture and in *ex vivo* infected macrophages (Burchmore *et al.*, 2003; Rodríguez-Contreras and Landfear, 2006; Rodriguez-Contreras *et al.*, 2007), while an *L. major* mutant lacking a key enzyme involved in the catabolism of exogenous amino sugars leads to loss of virulence in both *ex vivo* infected macrophages and in highly susceptible BALB/c mice (Naderer *et al.*, 2010).

Why *Leishmania* are dependent on sugars for intracellular survival remains unclear. *Leishmania* promastigotes and amastigotes constitutively express all of the enzymes needed

to utilize amino acids and gluconeogenesis suggesting that they could, in principle, switch to using amino acids as sole carbon sources (Rosenzweig *et al.*, 2008). The dependence of *Leishmania* amastigotes on sugar/amino-sugar catabolism could reflect stage-specific down-regulation of plasma membrane transporters involved in the uptake of NEAA, such as glutamate and aspartate, that can be catabolized in the TCA cycle and/or the availability of preferred amino acids in the phagolysosome. Alternatively, sugar metabolism could provide an adaptive advantage in the potentially oxidative environment of the phagolysosome niche.

Previous studies on the hexose transporter deficient *Δlmxgt1–3* mutant line have led to the identification of by-pass or suppressor mutant lines that have partially restored growth in glucose rich medium and infectivity in *ex vivo* infected macrophages (Feng *et al.*, 2013; Feng *et al.*, 2009). Biochemical analysis indicated that these lines had by-passed the need for LmxGT1–3 by up-regulating the expression of the permease, D2/LmxGT4, which can sustain some glucose uptake when overexpressed (Feng *et al.*, 2009). Here we report the characterization of a new *Δlmxgt1–3* suppressor line, Δ*lmxgt1–3*^{s2}, that exhibits a distinct adaptive response. In contrast to the previously reported suppressor line, *Δlmxgt1–3*^{s2} exhibits even lower rates of glucose uptake than the parental mutant, which is compensated by enhanced capacity to catabolize glutamate and aspartate as major carbon sources. This metabolic switch leads to increased intracellular growth in macrophages but does not restore virulence in mice. We show that the switch to amino acid catabolism and increased dependency on mitochondrial metabolism, in both promastigotes and amastigotes, leads to elevated levels of reactive oxygen species (ROS) and increased sensitivity to nitric oxide (NO). These data suggest that *Leishmania* amastigotes can use amino acids as major carbon sources in non-activated macrophages, but are restricted to using sugars (and to a lesser extent fatty acids) as major carbon sources in the pro-inflammatory environment of tissue lesions.

Results

Identification of a novel L. mexicana *glucose transporter suppressor mutant,* Δlmxgt1–3^{s2}

As previously reported (Burchmore *et al.*, 2003), promastigote stages of the *L. mexicana* Δ*lmxgt1–3* mutant lacking the three hexose transporters, LmxGT1–3, grow more slowly than wild type parasites when cultivated in standard RPMI medium containing 12 mM glucose and reach a lower final density in stationary phase (Fig 1A). The *Δlmxgt1–3* promastigotes also exhibit enhanced thermosensitivity compared to wild type parasites, and are unable to survive when cultivated at 33 °C in low pH medium. Under these conditions, wild type promastigotes differentiate to small, amastigote-like forms which lack an emergent flagellum, while the *Δlmxgt1–3* promastigotes retain their flagellum, swell up and eventually lyse (Fig 1B,C). The increased thermosensitivity of the *Δlmxgt1–3* mutant is also associated with a severe defect in the capacity of promastigotes to survive in *ex vivo* infected macrophages. *Δlmxgt1–3* promastigotes are internalized by RAW macrophages at the same rate as wild type parasites (data not shown) but are unable to proliferate within these host cells (Fig 2A). The *Δlmxgt1–3* line was also unable to induce lesions in highly susceptible BALB/c mice (Fig 2B, C) and viable parasites could not be recovered from either the site of infection (skin) or adjacent lymph nodes (Fig 2C).

Continuous culture of the *Δlmxgt1–3* mutant in rich medium can lead to the appearance of suppressor strains that overgrow the *Δlmxgt1–3* parasites (Feng *et al.*, 2009). Using this approached we isolated a new suppressor line, termed *Δlmxgt1–3^{s2}*, which exhibited significantly faster growth rates than *Δlmxgt1–3* promastigotes in RPMI medium (Fig 1A). This parasite line had a smaller cell body compared to wild type parasites, but was otherwise identical morphologically (Fig S1). In contrast to the parental mutant line, *Δlmxgt1–3^{s2}* promastigotes differentiated normally to amastigotes when suspended in low pH medium and cultivated at 33 °C (Fig 1B, C). *Δlmxgt1–3^{s2}* amastigotes also infected both RAW and J774 macrophages and proliferated at similar or faster rates than wild type parasites in these host cells (Fig 2A). In marked contrast, the virulence of *Δlmxgt1–3^{s2}* parasites was not restored in the murine model (Fig 2C). Specifically, infection with 10^8 parasites did not lead to the formation of lesions in BALB/c mice over >6 months. While biopsy of tissues and adjacent lymph nodes indicated that some *Δlmxgt1–3^{s2}* amastigotes can persist long term in both tissues, the parasite load was approximately 7 to 8 orders of magnitude lower than wild type parasites (Fig 2B).

The Δ*lmxgt1–3^{s2}* suppressor line does not exhibit restored glucose uptake.

To investigate whether the restored growth of *Δlmxgt1–3^{s2}* promastigotes and amastigotes in rich medium and macrophages, respectively, reflected restored hexose transport in the suppressor line, rates of glucose transport were measured in wild type and mutant promastigotes. Both *Δlmxgt1–3* or *Δlmxgt1–3^{s2}* promastigotes exhibited very low rates of hexose uptake in short term ^{14}C-glucose-labeling studies (Fig 3A). The residual rates of glucose uptake in both lines (approximately 50-fold lower than in wild type promastigotes) may reflect the activity of the low affinity hexose transporter, D2/LmxGT4 which is up-regulated in the *Δlmgt1–3 ^{s2}* line (Feng *et al.*, 2009).

We next tested whether *Δlmxgt1–3^{s2}* promastigotes compensate for reduced hexose up-take by increasing the activity of down-stream glycolytic enzymes. Wild type, *Δlmxgt1–3* and *Δlmxgt1–3^{s2}* promastigotes were labeled with ^{13}C-U-glucose over 12 hours and rates of glucose uptake and secretion of key metabolic end-products of glycolysis and glycosomal succinate fermentation were monitored by ^{13}C-NMR. Consistent with the short-term ^{14}C-glucose uptake experiments, both *Δlmxgt1–3* and *Δlmxgt1–3^{s2}* promastigotes exhibited reduced rates of ^{13}C-U-glucose uptake and secretion of major metabolic end-products compared to wild type parasites. Strikingly, uptake of ^{13}C-glucose (Fig 3B) and the turnover of intracellular pools of glucose 6-phosphate (Fig 3C) were significantly lower in the *Δlmxgt1–3^{s2}* suppressor mutant compared to the parental *Δlmxgt1–3* promastigotes. Similarly, direct measurement of glycolytic flux in wild type and the two mutants lines using the Seahorse metabolic analyzer showed that rates of glycolysis in *Δlmxgt1–3* and *Δlmxgt1–3^{s2}* promastigotes were significantly lower than in wild type parasites (Fig 3D). Interestingly, the rates of extracellular acidification (ECAR) were slightly higher in *Δlmxgt1–3^{s2}* promastigotes compared to *Δlmxgt1–3* promastigotes (Fig 3D). While ECAR is generally assumed to reflect the level of glycolysis, elevated ECAR can occur due to secretion of organic acid end-products. As shown below, the suppressor line has a more active TCA cycle, which could lead to secretion of TCA derived dicarboxylic acid intermediates that are not labeled with ^{13}C-glucose.

To further investigate the extent to which the *Δlmxgt1–3*^{s2} promastigotes utilize glucose, wild type and mutant lines were labeled with ^{13}C-U-glucose for 3 hours and ^{13}C-enrichment of key intermediates in central carbon was assessed by GC-MS. As expected, ^{13}C-glucose labeling of wild type promastigotes leads to high levels of ^{13}C-enrichment in intermediates in glycolysis, the pentose phosphate pathway, glycosomal succinate fermentation and small oligosaccharides representative of the carbohydrate reserve material, mannogen (CHO1/CHO2) (Fig 3E) (Saunders *et al.*, 2011; Saunders *et al.*, 2014). ^{13}C-enrichment is also observed at lower levels in intermediates in the tricarboxylic acid (TCA) cycle and interconnected amino acids, such as alanine, aspartate and glutamate. No label was detected in other NEAA (Gly, Thr, Ser) indicating that these amino acids are largely salvaged from the medium (Saunders *et al.*, 2011; Saunders *et al.*, 2014). Consistent with the global ^{13}C-NMR flux analysis, levels of ^{13}C-enrichment in intermediates in all metabolic pathways was reduced in ^{13}C-glucose -fed *Δlmxgt1–3* and further decreased in *Δlmxgt1–3*^{s2} promastigotes. In particular, ^{13}C-glucose flux into mitochondrial intermediates (citrate, malate and fumarate) as well as anaplerotically synthesized glutamate and aspartate was markedly reduced in the suppressor line (Fig 3E). Strikingly, steady-state levels of mannogen were restored to wild type levels in suppressor line (Fig S2) indicating a switch to utilization of alternative carbon sources and increased flux through gluconeogenesis. These analyses suggest that *Δlmxgt1–3*^{s2} promastigotes are metabolically adapted to using other carbon sources in the medium, which confers a strong growth advantage under standard *in vitro* growth conditions and in *ex vivo* infected macrophages, but not in mice infections.

The Δ*lmgt*^{s2} suppressor line exhibits enhanced catabolism of glutamate.

Leishmania can catabolize both fatty acids and amino acids, although only the carbon skeletons of amino acids can be used to sustain net gluconeogenesis due to the absence of a functional glycoxylate cycle in these parasites (McConville and Naderer, 2011). To investigate whether *Δlmxgt1–3*^{s2} promastigotes exhibit increased amino acid uptake, wild type, *Δlmxgt1–3* and *Δlmxgt1–3*^{s2} promastigotes were suspended in completely defined medium (CDM) containing a cocktail of ^{13}C-amino acids for 24 hours and the rate of catabolism in the TCA cycle determined by ^{13}C-NMR quantitation of ^{13}C-bicarbonate the culture medium. Rates of ^{13}C-bicarbonate production were increased in *Δlmxgt1–3* promastigotes (~2-fold) and even further in *Δlmgt*^{s} promastigotes (~3.5-fold) compared to wild type promastigotes (Fig 4A). Detailed analysis of intracellular metabolites of different parasite lines labeled with this cocktail indicated that the increased rate of catabolism of these amino acids was not due to a global increase in amino acid uptake, with rates of amino acid turnover being generally less than in wild type parasites (Fig S3). We have previously shown that *L. mexicana* promastigotes co-utilize alanine, aspartate and glutamate in the presence of glucose (Saunders *et al.*, 2011). To investigate whether these amino acids are preferentially utilized in the *Δlmxgt1–3*^{s2} mutant, wild type, *Δlmxgt1–3* and *Δlmxgt1–3*^{s2} promastigotes were metabolically labeled with ^{13}C-U-alanine, ^{13}C-U-aspartate or ^{13}C-U-glutamate in CDM. Consistent with previous studies, wild type parasites exhibited low rates of uptake and catabolism of alanine, aspartate and glutamate (Fig 4B). The minimal uptake of alanine likely reflects high secretory flux of this amino acid under conditions of high glucose utilization. While alanine uptake was increased in the *Δlmxgt1–3* mutant and *Δlmxgt1–3*^{s2} suppressor line, the further catabolism of this amino acid in the TCA cycle and

in gluconeogenesis was low (Fig 4B). In contrast, the uptake and catabolism of aspartate and glutamate was increased in *Δlmxgt1–3* promastigotes and further elevated in the *Δlmxgt1–3^{s2}* suppressor line (Fig 4B). Significantly, label in ^{13}C-U-glutamate-fed *Δlmxgt1–3* and *Δlmxgt1–3^{s2}* parasite lines was primarily shunted into TCA cycle intermediates downstream of α-ketoglutarate, with minimal labeling of citrate, indicating high rates of cataplerotic export of malate for gluconeogenesis and/or biomass production. The increased labeling of hexose-phosphates in the ^{13}C-glutamate-fed *Δlmxgt1–3^{s2}* promastigotes did not appear to reflect increased expression or activity of enzymes in the gluconeogenic pathways, as ^{13}C-glycerol was incorporated into glucose-6-phosphate with equal efficiency in both mutant lines (Fig 4C). These analyses suggest that *Δlmxgt1–3^{s2}* promastigote stages compensate for loss of LmxGT1–3 expression by increasing glutamate/aspartate uptake and catabolism, providing carbon skeletons for gluconeogenesis and ATP synthesis via mitochondrial oxidative phosphorylation.

The determine whether glutamate and/or aspartate equally supported mitochondrial metabolism and gluconeogenesis in *Δlmxgt1–3^{s2}*, promastigotes were cultivated in glucose-free CDM containing different non-essential amino acids (NEAA). As expected, wild type promastigotes were unable to grow in glucose free-CDM lacking NEAA (Fig 4D). Supplementation of this medium with glutamate, but not with aspartate, proline, or alanine alone (all at 6 mM) completely restored growth (Fig 4D). The inability of promastigotes to utilize aspartate or alanine as sole carbon sources in the absence of glucose may reflect exhaustion of critical pools of α-ketoacids, such as α-ketoglutarate during their transamination and with concomitant disruption of TCA cycle fluxes. *Δlmxgt1–3^{s2}* promastigotes was also only able to utilize glutamate as sole carbon sources in the absence of glucose but exhibited elevated growth compared to wild type promastigotes in glutamate-only medium (Fig 4D). These data are consistent with more efficient partitioning of glutamate carbon backbones into key energy-generating pathways and/or gluconeogenesis in the suppressor line.

Δlmxgt1–3^{s2} amastigotes also exhibit increased amino acid catabolism

We have previously shown that *L. mexicana* amastigotes enter into a slow growth, metabolically quiescent state in which overall rates of glucose uptake and catabolism are greatly reduced (Saunders *et al.*, 2014; Kloehn *et al.*, 2015). However, these stages are still dependent on the catabolism of sugars for the synthesis of carbon skeletons for key amino acids, such as glutamate. To investigate whether *Δlmxgt1–3^{s2}* amastigotes exhibit a similar hardwired metabolic response, wild type and *Δlmxgt1–3^{s2}* promastigotes were induced to differentiate to amastigotes and then labeled with ^{13}C-U-glucose, ^{13}C-U-aspartate and ^{13}C-U-glutamate for 3 hours (Fig. 5A). As expected, wild type axenic amastigotes (Ama^{axenic}) predominantly utilized ^{13}C-U-glucose as major carbon source, with concomitant ^{13}C-enrichment in all intermediates in glycolysis, the pentose phosphate pathway, succinate fermentation (Fig 5A) and mannogen (data not shown). Significant labeling of NEAA (alanine, aspartate and glutamate) was also observed in ^{13}C-U-glucose-fed wild type amastigotes. ^{13}C-enrichment in these amino acids was higher than in ^{13}C-U-aspartate and ^{13}C-U-glutamate-fed amastigotes consistent with *de novo* synthesis of these amino acids predominating over salvage (Fig 5A). In marked contrast, *Δlmxgt1–3^{s2}* Ama^{axenic} exhibited

negligible levels of ^{13}C-U-glucose uptake or labeling of intermediates in central carbon metabolism (Fig 5A), confirming the lack of any compensatory mechanism for salvaging sugars in the amastigote stage of the suppressor line. On the other hand, *Δlmxgt1–3*^{s2} amastigotes exhibited enhanced uptake of both ^{13}C-U-aspartate and ^{13}C-U-glutamate, which were catabolized in the TCA cycle (Fig 5A). Low levels of ^{13}C-enrichment in sugar phosphates were observed in *Δlmxgt1–3*^{s2} amastigotes reflecting the short labeling time and large pool of unlabeled mannogen in these cells which is constitutively mobilized to generate unlabeled hexose-phosphates. Bone marrow derived macrophages contain high levels of glutamate and aspartate (Fig 5C) supporting the notion that these amino acids might be available as carbon sources for intracellular amastigotes.

To confirm that intracellular *Δlmxgt1–3*^{s2} amastigotes are able to utilize non-sugar carbon sources in the macrophage phagolysosome, we measured levels of mannogen in these stages. Mannogen levels provide a measure of the bioenergetic state of *Leishmania* promastigotes and amastigotes, accumulating under conditions of hexose-phosphate excess and being depleted under conditions of hexose-phosphate limitation (Ralton *et al.*, 2003). As shown in Fig 5B, intracellular *Δlmxgt1–3*^{s2} amastigotes expressed similar levels of mannogen oligomers as wild type amastigotes. The predominance of mannogen oligomers with low degree of polymerization (dp) in wild type and *Δlmxgt1–3*^{s2} amastigotes is indicative of high rates of turnover (Ralton *et al.*, 2003). Thus intracellular *Δlmxgt1–3*^{s2} amastigotes, like promastigotes, appear to have switched to using amino acids as their major carbon source. Strikingly, supplementation of the medium of infected bone marrow derived macrophages (6 mM aspartate and glutamate) resulted in a significant increase in both wild type and *Δlmxgt1–3*^{s2} parasite burden in these host cells, particularly after seven days infection (Fig 5D). In contrast, addition of exogenous glutamate/aspartate did not enhance intracellular growth of *Δlmxgt1–3* parasites at this time point (Fig 5D). These data suggest that glutamate/aspartate levels in the phagolysosome of infected macrophages are limiting for intracellular growth of both wild type and Δlmxgt1–3^{s2} parasites.

Δlmgt1–3^{s2} amastigotes exhibit increased sensitivity to nitrosative stress

While the metabolic adaptations of *Δlmxgt1–3*^{s2} promastigotes and amastigotes promotes parasite growth in rich medium and in macrophages, these adaptations did not restore virulence in mice. We hypothesized that the switch to increased use of amino acids by intracellular amastigotes would lead to increased dependency on mitochondrial metabolism and elevated levels of endogenous reactive oxygen species formation, which may compromise parasite viability in animal infections. To confirm that intracellular *Δlmxgt1–3*^{s2} amastigotes are indeed dependent on an active mitochondrial metabolism, bone marrow derived macrophages were infected with wild type or *Δlmxgt1–3*^{s2} parasites in the presence or absence of 1 mM or 10 mM sodium fluoroacetate (NaFAc), a competitive inhibitor of the TCA cycle enzyme aconitase (Saunders *et al.*, 2011). As expected, intracellular growth of wild type parasites was only modestly affected by 1 or 10 mM NaFAc during the first four days of infection, although 10 mM NaFAc led to effective clearance of parasites by day 6 (Fig 6A). In contrast, growth of *Δlmxgt1–3*^{s2} amastigotes was severely restricted in the presence of 10 mM NaFAc at day 1 and by 1 mM at day 4 (Fig 6A).

The increased dependence of *Δlmxgt1–3*^{s2} parasites on mitochondrial metabolism was associated with increased basal levels of ROS, as detected by staining with DCFDA. Notably, levels of ROS in *Δlmxgt1–3*^{s2} promastigotes was 2-fold higher than in wild type parasites and 1.5-fold higher than in the parental *Δlmxgt1–3* mutant (Fig 6B). ROS levels increased in all parasite lines in the presence of hydrogen peroxide (data not shown) or menadione (Mittra et al., 2013) but remained higher in both the *Δlmxgt1–3* and *Δlmxgt1–3*^{s2} parasite lines (Fig 6B). These findings suggest that increased mitochondrial oxidative phosphorylation in the mutant lines leads to elevated levels of endogenous ROS production, contributing to the loss of virulence of both *Δlmxgt1–3* and *Δlmgt1–3*^{s2} parasite lines in mice.

Recent studies have shown that *Leishmania* amastigotes are exposed to sub-lethal concentrations of nitric oxide in inflammatory lesions (Müller *et al.*, 2013). NO is known to be a potent inhibitor of multiple enzymes in the mitochondrial TCA cycle, which may explain why *Leishmania* amastigotes normally depend primarily on hexose metabolism for growth *in vivo*, and enter the slow growth metabolically quiescent state (McConville *et al.*, 2015). To investigate whether *Δlmxgt1–3*^{s2} Ama^{axenic} are more susceptible to NO than wild type parasites, both lines were cultivated in the presence of different concentrations of $NaNO_2$ (which is converted to NO under acidic conditions (Alspaugh and Granger, 1991)) and amastigote viability measured by FACS analysis of eFluor-stained cells. While wild type amastigotes were relatively resistant to 2 mM $NaNO_2$, *Δlmxgt1–3*^{s2} amastigotes rapidly lost viability at this concentration (Fig 6C). Wild type amastigotes were resistant to $NaNO_2$ regardless of whether they were cultivated under glucose-replete or glucose-limiting conditions, reflecting the limited capacity of non-adapted wild type amastigotes to switch to catabolizing amino acids in the TCA cycle. *Δlmxgt1–3*^{s2} amastigotes were partially protected from NO toxicity by addition of 12 mM glucose, supporting the notion that toxicity is due to elevated mitochondrial respiration in the suppressor line. To confirm that NO does indeed inhibit mitochondrial respiration in the *Δlmxgt1–3*^{s2} amastigotes, wild type and *Δlmxgt1–3*^{s2} amastigotes were labeled with ^{13}C-U-glutamate or ^{13}C-U-fatty acids in the presence or absence of $NaNO_2$. In both cases, $NaNO_2$-treatment led to a marked decrease in the level of ^{13}C-enrichment in all TCA cycle intermediates (Fig 6D). Interestingly, $NaNO_2$ treatment also led to decreased uptake of glutamate which could reflect the impact of decreased mitochondrial ATP synthesis on cellular levels of ATP and ion transport fluxes in amastigotes. Finally, inhibition of mitochondrial metabolism was associated with an increase in ROS in $NaNO_2$-treated Ama^{axenic} (Fig 6E).

To more directly test whether host cell derived NO or ROS contributes to the severe-loss of virulence phenotype of *Δlmxgt1–3*^{s2} parasites in mice, infected bone marrow derived macrophages were stimulated with either lipopolysaccharide (LPS) alone or in combination with interferon gamma (IFNγ) (Fig 6F). These treatments activate NO and ROS synthesis in macrophages and resulted in partial restriction of growth of wild type parasites (Fig 6F). In contrast, activation of macrophages with LPS or LPS/INFγ resulted in almost complete clearance of *Δlmxgt1–3*^{s2} parasites. Compensatory up-regulation of amino acid catabolism in *Δlmxgt1–3*^{s2} amastigotes may therefore lead to increased vulnerability to endogenous and exogenous reactive oxygen/nitrogen species, accounting for the loss of virulence phenotype of the suppressor strain in mice.

Discussion

We have identified a novel suppressor line of *L. mexicana Δlmxgt1–3* in which the defect in glucose uptake is by-passed by increased catabolism of NEAA. This suppressor line was subsequently used to investigate the relationship between amastigote metabolism and capacity to survive in the phagolysosome compartment of *ex vivo* infected macrophages and in infected tissues. Unexpectedly, we show that while the *Δlmxgt1–3*^{s2} line can grow in non-activated macrophages, this line is highly attenuated in activated macrophages and exhibits a severe loss of virulence in mice. These data suggest that the macrophage phagolysosome contains sufficient amino acids to sustain amastigote growth, but that utilization of respiratory carbon sources increases the sensitivity of amastigotes to host microbicidal processes such as ROS and reactive nitrogen species. These findings are consistent with previous studies showing that *Leishmania* amastigotes preferentially utilize sugars as carbon source and normally exhibit very low rates of amino acid utilization. These metabolic adaptations are part of a coordinated metabolic quiescence, or stringent response, which likely represents a critical adaption to life in the macrophage phagolysosome.

The *Δlmxgt1–3*^{s2} suppressor line was isolated after selection of *Δlmxgt1–3* promastigotes for faster growth in rich medium and subsequent clonal isolation. Detailed ^{13}C-labeling studies suggested that the faster growth of these promastigotes in standard rich medium was not due to restoration of glucose uptake, but rather to increased catabolism of NEAA. This phenotype was particularly evident in *Δlmxgt1–3*^{s2} amastigotes which showed negligible rates of ^{13}C-U-glucose utilization, but increased rates of ^{13}C-U-glutamate and ^{13}C-U-aspartate catabolism. We have previously shown that wild type amastigotes also display increased rates of fatty acid β-oxidation compared to promastigotes (Saunders *et al.*, 2014). *Δlmxgt1–3*^{s2} amastigotes also catabolized ^{13}C-U-fatty acid, although the rate of utilization was considerably less than for ^{13}C-amino acids. The suppressor line was also hypersensitive to the TCA cycle inhibitor, sodium fluoroacetate, and exhibited high basal levels of ROS, both consistent with increased dependence on mitochondrial metabolism. As summarized in Fig 7, this switch to increased amino acid and mitochondrial metabolism is likely to be essential for ATP synthesis and supply of carbon skeletons for gluconeogenesis.

The precise molecular basis for increased catabolism of NEAA in *Δlmxgt1–3*^{s2} promastigotes and amastigotes remains undefined. While it is possible that expression of plasma membrane amino acid transporters is increased in the suppressor strain, we did not observe increased uptake of NEAA or essential amino acids. It is therefore likely that the increased uptake of specific NEAA (Glu, Asp, Ala) is driven by increased catabolism and depletion of intracellular pools of these amino acids. Interestingly, while it is commonly assumed that *Leishmania* preferentially utilize proline as an alternative carbon source under glucose limiting conditions, neither wild type nor mutant parasite lines exhibited appreciable rates of proline uptake and catabolism (Fig S3) or capacity to survive on this amino acid as sole carbon source in CDM. In principal, *Δlmxgt1–3*^{s2} parasites could also acquire amino acids via increased lysosomal degradation of extracellular proteins. However, labeling studies on wild type and *Δlmxgt1–3*^{s2} amastigotes with ^{13}C-algal proteins did not lead to significant ^{13}C-enrichment in intracellular metabolites (data not shown) indicating that amino acid uptake via surface transporters is the major route of acquisition. Similarly, both

Δlmxgt1–3 and *Δlmxgt1–3*^{s2} lines exhibited similar rates of gluconeogenesis when provided with ^{13}C- glycerol indicating that the final steps in this pathway are not up-regulated in the suppressor mutant.

It is likely that the *Δlmxgt1–3*^{s2} parasites have undergone multiple genetic changes since the generation of the original mutant. Specifically, the parental *Δlmxgt1–3* line used in this study, already exhibited significant levels of glucose uptake compared to the original *Δlmxgt1–3* (Burchmore et al 2003) which may reflect increased expression of the low affinity transporter, LmxGT4 (Feng et al 2009). Interestingly, the suppressor line exhibited lower rates of glucose uptake than the parental line, which may reflect loss of extra-chromosomal element carrying LmxGT4 and/or increased flux through gluconeogenesis driven by changes in mitochondrial metabolism. Further studies will be needed to define the potential contribution of changes in gene dosage (amplification/loss), gene mutations or post-transcriptional mechanisms in driving these metabolic adaptations.

While the *Δlmxgt1–3* parasites grow slowly in *ex vivo* infected macrophages and are eventually cleared, *Δlmxgt1–3*^{s2} amastigotes grow at a similar or faster rate than wild type amastigotes in a variety of non-activated macrophage lines (J7741.A, RAW, murine bone marrow derived macrophages). This intracellular phenotype suggests that levels of NEAA in the phagolysosome of non-activated macrophages are sufficient to sustain elevated rates of amastigote replication. Interestingly, supplementation of the growth medium of infected macrophages with additional glutamate/aspartate (6 mM each) stimulated the intracellular growth of both wild type and the suppressor line parasites. Thus intracellular amastigote group may be partially constrained by the availability of NEAA in the phagolysosome, although it is also possible that exogenous NEAA may directly or indirectly induce other changes in macrophage metabolism that benefit amastigote survival and proliferation.

In contrast to the situation in cultured macrophages, we show for the first time that neither the *Δlmxgt1–3* or *Δlmxgt1–3*^{s2} lines induced lesions in BALB/c mice. Some *Δlmxgt1–3*^{s2}, but not *Δlmxgt1–3* parasites were recovered from the site of injection and in proximal lymph nodes, indicating that the metabolic adaptations observed in the latter line may confer a slight advantage over the parental line. Independent infection experiments with several different clones of *Δlmxgt1–3* in one of our laboratories (S.M.L, unpublished data) confirmed the highly-attenuated virulence phenotype of this strain, although small lesions were observed when BALB/c mice were injected in the footpad. These subtle differences may reflect cross-laboratory differences in the strains and/or the site of injection (tail versus footpad) used. Regardless, the highly-attenuated virulence of *Δlmxgt1–3*^{s2} in mice contrasted dramatically with the prolific intracellular growth of this line in *ex vivo* infected macrophages. There are a number of possible reasons for why the metabolic switch in the *Δlmxgt1–3*^{s2} line may not lead to effective rescue of amastigote growth in mice compared to *ex vivo* infected macrophages. First, the phagolysosomes of macrophages in inflammatory lesions may contain lower levels of NEAA needed to sustain the growth and viability of this parasite lines, compared to macrophages cultured in rich medium. This possibility is supported by the finding that addition of exogenous NEAA to infected macrophages increased parasite growth. However, as noted above, *L. mexicana* amastigotes can also scavenge amino acids from the proteolytic breakdown of host proteins in their own

lysosomes and are therefore not necessarily dependent on amino acids levels in the phagolysosome (Besteiro *et al.*, 2007). A second possibility is that *Δlmxgt1–3*^{s2} amastigotes are more sensitive than wild type amastigotes to increased levels of ROS and/or NO in the lesion microenvironment (Müller *et al.*, 2013). Consistent with this possibility we show that axenic *Δlmxgt1–3*^{s2} amastigotes are highly sensitive to NO and that intracellular *Δlmxgt1–3*^{s2} amastigotes are effectively cleared by LPS or LPS/IFNγ activated macrophages. Mitochondrial enzymes containing iron-sulphur clusters in the TCA cycle and respiratory chain complexes are highly vulnerable to inactivation by ROS and nitrosylation and exposure of *Δlmxgt1–3*^{s2} amastigotes to NO leads to complete inhibition of amino acid catabolism. The increased dependency of *Δlmxgt1–3*^{s2} amastigotes on amino acid catabolism and mitochondrial respiration may therefore increase the sensitivity of this line to sub-lethal production of NO in infected tissues (Müller *et al.*, 2013) and constrain proliferation. Unexpectedly, ectopic expression of individual LmGT transporters (LmGT2-GFP and LmGT3-GFP) in the suppressor line did not protect this line from being cleared in LPS-activated macrophages (unpublished data). The failure to restore intracellular growth in activated macrophages could reflect partial restoration of hexose uptake in these complemented lines (Vince et al 2011). Alternatively, complex metabolic changes in the suppressor line may have led to amino acids being the preferred carbon source under a wide range of growth conditions.

While our results suggest that a switch from glycolysis to increased dependence on mitochondrial respiration is strongly detrimental for *Leishmania* pathogenesis, other pathways associated with catabolism of non-sugar carbon sources may still be important in intracellular stages. Specifically, we have previously shown that *L. major* amastigotes are dependent on expression of the gluconeogenic enzyme, fructose-1,6-bisphosphatase (FBPase) for growth in macrophages and infectivity in mice (Naderer *et al.*, 2006). FBPase catalyzes the last step in gluconeogenesis and could be involved in maintaining steady-state hexose-phosphate levels, either through the conversion of carbon skeletons derived from amino acids to sugar phosphates or by regulating the flux of hexose-phosphates in upper glycolysis. In support of the latter possibility, we have recently shown that intracellular *Toxoplasma gondii* tachyzoites are dependent on expression of FBPase while using glucose as major carbon source to sustain high glycolytic flux (Blume *et al.*, 2015).

Amastigote differentiation is associated with induction of the stringent metabolic response, whereby amastigotes strongly repress their utilization of both sugars and amino acids, minimize overflow metabolism (i.e. secretion of partially oxidized end-products) and primarily utilize the TCA cycle for anabolic reactions, such as synthesis of NEAA (Saunders *et al.*, 2014). Our findings suggest that induction of the stringent metabolic response may have a number of functions. Specifically, the slow growth (12 day doubling time, (Kloehn *et al.*, 2015)) and low metabolic requirements of this stage would minimize the risk of overgrowing this intracellular niche and reduce the need to use carbon sources other than sugars. Entry into this state would also minimize mitochondrial metabolism in intracellular amastigote stages thereby reducing the vulnerability of these stages to macrophage NO and ROS production. A similar response is induced in amastigotes cultured under nutrient rich conditions (Saunders *et al.*, 2014) suggesting that this response is both hardwired and has a strong adaptive advantage to intracellular amastigotes.

These studies suggest that *Leishmania* amastigotes have limited capacity to develop resistance to inhibitors of hexose uptake and catabolism in the glycolytic pathway, as metabolic adaptations that lead to increased utilization of other carbon sources and mitochondrial metabolism will increase their sensitivity to host microbicidal processes. Paradoxically, the dependence of *Leishmania* amastigotes on sugars as their major carbon source, and down-regulation of NEAA uptake, means that these stages are dependent on anapleurotic mitochondrial reactions involved NEAA biosynthesis. Indeed a number of studies have shown that inhibitors of mitochondrial metabolism have potent anti-leishmania activity (Fidalgo and Gille, 2011; Ortiz *et al.*, 2016; Saunders *et al.*, 2014). These studies suggest that *Leishmania* amastigote metabolism is highly constrained *in vivo*, which offers new opportunities for drug development.

Methods

Parasite strains and growth conditions- L. mexicana wild type (wild type) (MNYC/BZ/62/M379), *Δlmxgt1–3* and *Δlmxgt1–3*^{s2} promastigotes were cultured in RPMI 1640 medium (Sigma) supplemented with 10 % heat inactivated foetal calf serum (iFCS, GibcoBRL) at 27 °C. Parasites were passaged twice weekly (1/100 and 1/1000 dilutions) into fresh media to maintain log phase growth. Parasite proliferation was assessed using a haemocytometer. Stationary phase promastigotes were induced to differentiate to Ama^{axenic} by acidification of the conditioned media to pH 5.5 with HCl, and supplementation with an additional 10 % iFCS (20 % iFCS final) and subsequent cultivation at 33 °C for 5 days. For amino acid growth dependency experiments, promastigotes were suspended in glucose-free completely defined medium (Glc-free CDM) lacking NEAA, with or without supplementation with individual amino acids (6 mM). To assess the susceptibility of Ama^{axenic} to NO, amastigotes were resuspended in glucose-free RPMI, 20% iFCS (pH 4.5, 2×10^7 cell/ml) supplemented with glucose (0, 6, 13 mM) and sodium nitrite (0, 0.5, 1, 2 mM) (Alspaugh and Granger, 1991). For microscopy, parasites were incubated in 4 % paraformaldehyde (in PBS) for 10 min and then added to poly-L-lysine treated coverslips. Cells were visualised by DIC microscopy using the Axioplan 2 imaging microscope equipped with AttoArc 2, HBO 100 Arc Lamp Control (Zeiss).

Parasite viability- L. mexicana wild type, *Δlmxgt1–3* and *Δlmxgt1–3*^{s2} amastigotes were washed once with PBS and then incubated in propidium iodide (0.2 ug/ml in PBS) for 10 min. The parasites were pelleted (15,000 x *g*, 30 min) then washed a further two times with PBS before being applied to coverslips and visualised by fluorescence microscopy (488 nm excitation). Microscopy was performed on the Axioplan 2 imaging microscope equipped with AttoArc 2, HBO 100 Arc Lamp Control (Zeiss). Images were collected using the Axiovision software. Alternatively, parasite viability was assessed by FACS analysis after Ama^{axenic} were washed twice with PBS, then stained with the fixable viability dye, eFluor 520 (eBioscience, 65–0867, 5×10^6 cell total in 1 ml 1xPBS with 1 µl dye, 30 min, 2–8 °C). Parasites were washed, fixed (4 % PFA, 500 uL, 30 min), washed, and then resuspended in PBS (5×10^6 cell/500 µL) for FAC analysis. Flow cytometry results were acquired on a FACSort (BD) and data analysed with the FloJo software package.

Glucose uptake assay - Aliquots *L. mexicana* wild type, *Δlmxgt1–3* and *Δlmxgt1–3*^{s2} mid log phase promastigotes (6×10^7 cells total) were washed twice in PBS with intermediate centrifugation (30 sec, 14,000 x *g*). The cell pellets were immediately suspended in 200 μl of either RPMI medium (pH 7.4) containing 0.2 mM glucose. An aliquot of the cell suspension (50 μl) was added to PCR tube and the uptake assay initiated by the addition of 50 μl of RPMI medium, prewarmed to 27°C, containing ^{14}C-U-glucose (308 mCi/mmol, 10 μCi/assay). The cell suspension (100μl) was layered over an oil cushion (dibutyl phthalate:mineral oil, 9:1 v/v, 50 μl) at 30, 45 and 60 sec, and centrifuged (30 sec, 14,000 x *g*) to pellet labelled cells. The upper phase was washed twice with PBS to remove excess radiolabel and the oil-phase was then removed and the cell pellet resuspended in 0.5 % SDS (250 μl). After sonication, the lysate (200 μl) was mixed with scintillation fluid (2 ml) and radioactivity determined by scintillation counting.

Stable isotope labeling experiments - Parasite lines were labeled with different ^{13}C-labeled carbon sources as described in (Saunders *et al.*, 2014; Saunders *et al.*, 2011) . Briefly, kinetic labeling studies promastigotes (in mid log phase) were washed and resuspended in glucose-free RPMI medium and aliquoted into ten 15 mL screw cap tubes (4×10^7 cells per tube, one tube for each time point) and incubated at 27 °C. Labeling was initiated by addition of 0.8 mM ^{13}C-U-glucose and parasites harvested at indicated time points by rapid chilling and centrifugation (Saunders *et al.*, 2011). For all other labeling experiments, promastigotes (mid-log phase) or Ama^{axenic} were resuspended in completely defined media (CDM, 2×10^7 cell/ml) containing various ^{13}C-labeled carbon sources. The composition of CDM, based on (Merlen *et al.*, 1999; Saunders *et al.*, 2011; Saunders *et al.*, 2014), contained glucose (6 mM), alanine (1.9 mM), arginine (0.4 mM), glycine (3.1 mM), histidine (0.04 mM), isoleucine (0.045 mM), leucine (0.61 mM), lysine (0.55 mM), methionine (0.13 mM), phenylalanine (0.18 mM), proline (0.26 mM), serine (0.76 mM), threonine (0.34 mM), tyrosine (0.033 mM), valine (1.1 mM) and tryptophan (0.15 mM), vitamins, heme and 0.5 % bovine serum albumin (BSA) containing bound fatty acids. For the labeling studies, naturally-labeled carbon sources were replaced with the following ^{13}C-U labeled carbon sources (Cambridge Stable Isotopes): ^{13}C-U-glucose (6 mM), ^{13}C-U-alanine (1.5 mM), ^{13}C-U-aspartate (1.5 mM), ^{13}C-U-glutamine (1.5 mM), ^{13}C-U-glutamate (1.5 mM), ^{13}C-U-proline (1.5 mM). For labeling experiments with ^{13}C-U-fatty acid, a cocktail of saturated/unsaturated ^{13}C-U-fatty acids coupled to delipidated bovine serum albumin were added to CDM. The ^{13}C-U-amino acid mix was used at 1 g/lit.

Metabolite extraction and GC-MS analysis – Metabolically quenched cells were pelleted, washed three times with chilled PBS and extracted in chloroform:methanol:water (1:3:1 v/v, 250 μl, containing 1 nmol *scyllo*-inositol internal standard) at 60 °C for 15 min with periodic mixing. Insoluble material was pelleted by centrifugation (16,100 x *g*, 5 min, 0 °C) and the supernatant was adjusted to chloroform:methanol:water (1:3:3 v/v) by the addition of H_2O. After vortex mixing and phase separation by centrifugation (16,000 x *g*, 5 min), the upper polar phase was transferred to GC vial inserts and dried *in vacuo* at 55 °C. Polar metabolites were methoximated (methoxyamine HCl, Supelco, 20 mg/mL, 20 uL in pyridine, overnight incubation) and derivitised (BSTFA+TMCS, 99:1, Supelco, 20 uL, 1–2 hr) prior to GC-MS analysis (Saunders *et al.*, 2014; Saunders *et al.*, 2011). Metabolite identification was performed in Chemstation (Agilent) and referencing authentic standards. Fractional labelling

and corrected mass isotopomer distributions (MID) were performed using in house DExSI software.

Macrophage infection - Bone marrow derived macrophages (BMM) were harvested from BALB/C mice (tibia and femur) and suspended RPMI media supplemented with 15 % iFCS, 20 % L cell media, penicillin (100 U/ml) and streptomycin (100 μg/mL) at 37 °C with 5 % CO_2 on TC plates. The following day, differentiating (but not adherent) macrophages were transferred to petri dishes and incubated at 37 °C with 5 % CO_2 and maintained for 5–7 days before being used. RAW macrophages were cultured in RPMI supplemented with 10 % iFCS and penicillin (100 U/ml) and streptomycin (100 μg/mL) at 37 °C with 5 % CO_2. Cells were passaged 2–3 times weekly by scraping adherent cells into fresh media and diluting a further 5-fold. Macrophages were maintained for no more than 10 passages. For imaging, macrophages were suspended in fresh RPMI 1640 supplemented with 10 % iFCS (and 20 % L cell media for primary macrophages), penicillin (100 U/ml) and streptomycin (100 μg/mL), aliquoted into 24-well plates containing 10 mm glass cover slips ($2–5 \times 10^5$ macrophages/ml, 0.5 mL per well) and allowed to adhere overnight (at 37 °C with 5 % CO_2). The following day, the macrophage monolayers were overlaid with stationary phase promastigotes or Ama^{axenic} (multitude of infection (MOI) 5:1 or 10:1). The cultures were incubated at 33 °C in 5 % CO_2 for 4 hours before non-adherent parasites were removed by washing the monolayers twice with PBS. For some experiments, the macrophage culture media was supplemented with additional aspartate/glutamate (6 mM, each) , lipopolysaccharaide (LPS, 10 ng/ml) and/or interferon gamma (IFNγ, 20 ng/ml). The cultures were maintained at 37°C with 5 % CO_2 for up to 7 days. Coverslips were removed at specified time points for microscopy. To enumerate levels of infection the monolayers were washed in PBS (three times), fixed in methanol (4 °C, 10 min) or 4 % paraformaldehyde (10 min) mounted in Hoechst containing Mowiol® 4–88 or Fluoromont (eBioscience). The percent infected cells and the number of parasites per cell were quantitated by fluorescence microscopy. Parasite index was determined by multiplying the number of amastigotes per macrophage by the percent of macrophage infected. Average and standard deviation were calculated from (at least) three independent replicates. All microscopy was performed on the Axioplan 2 imaging microscope equipped with AttoArc 2, HBO 100 Arc Lamp Control (Zeiss). Images were collected using the AxioVision software. To quantify amino acid abundance in infected and uninfected host cells, bone marrow derived macrophages were plated into a 6-well plate (5ml RPMI supplemented with 10 % iFCS, $2×10^6$ cell total) and incubated 37 °C overnight. Macrophages were infected with *L. mexicana* wild type promastigotes (MOI 5:1) for 24 hr, then rapidly washed with ice-cold PBS to quench metabolism. Adherent macrophages were extracted in ice-cold methanol (1.2 mL), prior to removal of residual cell material with a cell scaper and extraction of the cell pellet in chloroform:methanol:water (1:3:1 v/v). Polar metabolites were analysed by GC-MS as described above.

NMR analysis of carbon source uptake and metabolite secretion- wild type, *Δlmxgt1–3* and Δ*lmxgt1–3*^{s2} parasites were labeled for 24 hours, and the cell-free culture supernatant (540 μl) gently premixed with 5 mM D6-DSS in D_2O (60 μl, containing 0.2 % w/v NaN_3), 21.4 mM ^{13}C-U-glycerol in D_2O (5 μl, containing 0.2 % w/v NaN_3) and 21.4 mM imidazole in D_2O (5 μl, containing 0.2 % w/v NaN_3), prior to analysis by NMR. ^{13}C-spectra at 200 MHz

were obtained using an 800 MHz Bruker-Biospin Avance fitted with a cryoprobe (Saunders *et al.*, 2011).

Mannogen analysis - J774A.1 macrophages (20 ml, 75 cm^2) were infected by either wild type or *Δlmxgt*^{s2} stationary phase promastigotes (MOI 10:1) and incubated at 34 °C with 5 % CO_2. Five days after inoculation, uninfected and infected macrophages were extracted in hot water (100 °C, 10 min) and the soluble extract desalted on AG50(H^+)/AG3(OH^-) mixed bed resin and analyzed by high pH anion exchange liquid chromatography (HPAEC) (Ralton *et al.*, 2003).

Measurement of glycolytic fluxes- wild type, Δ*lmxgt1–3* and *Δlmxgt1–3*^{s2} mid log phase promastigotes were plated onto 96-well plates coated with Cell-Tak (Corning, 354240) (1.25 ×10^6 cell/well) in XF base media (80 uL/well), centrifuged and incubated at 27 °C for 30 min prior to assay. Extracellular acidification rates (ECAR) were monitored using the Seahorse Extracellular Flux (XF) Analyser (Agilent) upon sequential addition of the following carbon source/inhibitors; basal measurement (no injection), glucose (1 mM final, Port A), oligomycin (3 uM final, Port B), 2-deoxy glucose (50 mM final, Port C), antimycin A/rotanone (0.5 uM final, Port D).

Mouse infection - Female BALB/c mice (6–8 weeks old) were infected by subcutaneous injection of 2×10^6 stationary phase promastigotes in 50 μl of PBS at the base of the tail. Infections (5 mice per treatment) were measured by scoring the diameter of the resulting lesion (0 for no lesion up to 4 for a lesion greater than 10 mm in diameter) (Mitchell and Handman, 1983). To quantify parasite burden at the site of infection or in adjacent lymph nodes, mice were sacrificed by cervical dislocation and tissue amastigotes extracted aseptically as described previously without filtration. Samples were resuspended in 5 ml of PBS, aliquoted into a 96-well plate (250 μL/well) and serially diluted (1/10) in RPMI medium supplemented with 10 % iFCS. Parasite proliferation was measured by counting the number of parasites at the highest dilution.

Measurement of Reactive Oxygen Species (ROS) – ROS were detected using a plate based assay adapted from (Ortiz *et al.*, 2016; Mukherjee *et al.*, 2002). Briefly, log phase parasites were pelleted and resuspended in fresh RPMI supplemented with 10 % iFCS (400 uL, 1 × 10^7 cell/ml) in the presence of selected ROS-inducing compounds (H_2O_2 and menadione (MEN), 75 uM and 2.5 uM respectively) and incubated at 27 °C for 2 hrs. Cells were pelleted, resuspended in fresh RPMI media supplemented with 10% iFCS (400 μL) containing 20 μM H_2DCFDA (Sigma) and incubated in the dark at 27 °C for 30 min. Cells were then dispensed into a 96 well plate (100 μL/well, black walled, flat bottomed) and the plate analysed (CLARIOstar microplate reader) at excitation 485 and emission 535 nm. All measurements of fluorescence were corrected to unstained controls.

Supplementary Material

Refer to Web version on PubMed Central for supplementary material.

Acknowledgements

This work was supported by the Australian National Health and Medical Research Council. MJM is a NHMRC Principal Research Fellow. We acknowledge contributions by Dr William Ng, Dr Milica Ng and Dr Miriam Ellis to work that led up to this study.

References

Alspaugh JA, and Granger DL (1991) Inhibition of *Cryptococcus neoformans* replication by nitrogen oxides supports the role of these molecules as effectors of macrophage-mediated cytostasis. Infect Immun 59: 2291–2296. [PubMed: 2050398]

Besteiro S, Williams RAM, Coombs GH, and Mottram JC (2007) Protein turnover and differentiation in *Leishmania*. Int J Parasitol 37: 1063–1075. [PubMed: 17493624]

Blume M, Nitzsche R, Sternberg U, Gerlic M, Masters SL, Gupta N, and McConville MJ (2015) A *Toxoplasma gondii* Gluconeogenic Enzyme Contributes to Robust Central Carbon Metabolism and Is Essential for Replication and Virulence. Cell Host Microbe 18: 210–220. [PubMed: 26269956]

Burchmore RJS, Rodriguez-Contreras D, McBride K, Merkel P, Barrett MP, Modi G, et al. (2003) Genetic characterization of glucose transporter function in *Leishmania mexicana*. Proc Natl Acad Sci U S A 100: 3901–3906. [PubMed: 12651954]

Feng X, Rodriguez-Contreras D, Buffalo C, Bouwer HGA, Kruvand E, Beverley SM, and Landfear SM (2009) Amplification of an alternate transporter gene suppresses the avirulent phenotype of glucose transporter null mutants in *Leishmania mexicana*. Mol Microbiol 71: 369–381. [PubMed: 19017272]

Feng X, Rodriguez-Contreras D, Polley T, Lye L-F, Scott D, Burchmore RJS, et al. (2013) 'Transient' genetic suppression facilitates generation of hexose transporter null mutants in Leishmania mexicana. Mol Microbiol 87: 412–429. [PubMed: 23170981]

Fidalgo LM, and Gille L (2011) Mitochondria and trypanosomatids: targets and drugs. Pharm Res 28: 2758–2770. [PubMed: 21935742]

Kloehn J, Blume M, Cobbold SA, Saunders EC, Dagley MJ, and McConville MJ (2016) Using metabolomics to dissect host-parasite interactions. Curr Opin Microbiol 32: 59–65. [PubMed: 27200489]

Kloehn J, Saunders EC, O'Callaghan S, Dagley MJ, and McConville MJ (2015) Characterization of metabolically quiescent *Leishmania* parasites in murine lesions using heavy water labeling. PLoS Pathog 11: e1004683. [PubMed: 25714830]

McConville MJ, and Naderer T (2011) Metabolic Pathways Required for the Intracellular Survival of *Leishmania*. Annu Rev Microbiol 65: 543–561. [PubMed: 21721937]

McConville MJ, Saunders EC, Kloehn J, and Dagley MJ (2015) Leishmania carbon metabolism in the macrophage phagolysosome- feast or famine? F1000Res 4: 938. [PubMed: 26594352]

Merlen T, Sereno D, Brajon N, Rostand F, and Lemesre JL (1999) Leishmania spp: completely defined medium without serum and macromolecules (CDM/LP) for the continuous in vitro cultivation of infective promastigote forms. Am. J. Trop. Med. Hyg 60: 41–50. [PubMed: 9988320]

Mitchell GF, and Handman E (1983) *Leishmania tropica* major in mice: vaccination against cutaneous leishmaniasis in mice of high genetic susceptibility. Aust. J. Exp. Biol. Med. Sci 61: 11–25. [PubMed: 6870673]

Mukherjee SB, Das M, Sudhandiran G, and Shaha C (2002) Increase in cytosolic Ca2+ levels through the activation of non-selective cation channels induced by oxidative stress causes mitochondrial depolarization leading to apoptosis-like death in *Leishmania donovani* promastigotes. J Biol Chem 277: 24717–24727. [PubMed: 11983701]

Müller AJ, Aeschlimann S, Olekhnovitch R, Dacher M, Späth GF, and Bousso P (2013) Photoconvertible Pathogen Labeling Reveals Nitric Oxide Control of *Leishmania major* Infection In Vivo via Dampening of Parasite Metabolism. Cell Host Microbe 14: 460–467. [PubMed: 24139402]

Naderer T, Ellis MA, Sernee MF, De Souza DP, Curtis J, Handman E, and McConville MJ (2006) Virulence of *Leishmania major* in macrophages and mice requires the gluconeogenic enzyme fructose-1,6-bisphosphatase. Proc Natl Acad Sci U S A 103: 5502–5507. [PubMed: 16569701]

Naderer T, Heng J, and McConville MJ (2010) Evidence that intracellular stages of *Leishmania major* utilize amino sugars as a major carbon source. PLoS Pathog 6: e1001245. [PubMed: 21203480]

Naderer T, Heng J, Saunders EC, Kloehn J, Rupasinghe TW, Brown TJ, and McConville MJ (2015) Intracellular Survival of *Leishmania major* Depends on Uptake and Degradation of Extracellular Matrix Glycosaminoglycans by Macrophages. PLoS Pathog 11: e1005136. [PubMed: 26334531]

Ortiz D, Forquer I, Boitz J, Soysa R, Elya C, Fulwiler A, et al. (2016) Targeting the Cytochrome bc1 Complex of *Leishmania* Parasites for Discovery of Novel Drugs. Antimicrob Agents Chemother 60: 4972–4982. [PubMed: 27297476]

Pigott DM, Bhatt S, Golding N, Duda KA, Battle KE, Brady OJ, et al. (2014) Global distribution maps of the leishmaniases. Elife 3.

Ralton JE, Naderer T, Piraino HL, Bashtannyk TA, Callaghan JM, and McConville MJ (2003) Evidence that intracellular beta1–2 mannan is a virulence factor in *Leishmania* parasites. J Biol Chem 278: 40757–40763. [PubMed: 12902334]

Rodriguez-Contreras D, Feng X, Keeney KM, Bouwer HGA, and Landfear SM (2007) Phenotypic characterization of a glucose transporter null mutant in *Leishmania mexicana*. Mol Biochem Parasitol 153: 9–18. [PubMed: 17306380]

Rodríguez-Contreras D, and Landfear SM (2006) Metabolic changes in glucose transporter-deficient *Leishmania mexicana* and parasite virulence. J Biol Chem 281: 20068–20076. [PubMed: 16707495]

Rosenzweig D, Smith D, Opperdoes F, Stern S, Olafson RW, and Zilberstein D (2008) Retooling *Leishmania* metabolism: from sand fly gut to human macrophage. FASEB J 22: 590–602. [PubMed: 17884972]

Saunders EC, Ng WW, Chamber JM, Ng M, Naderer T, Kroemer JO, et al. (2011) Isoptopomer profiling of *Leishmania mexicana* promastigotes reveals important roles for succinate fermentation and aspartate uptake in TCA cycle anaplerosis, glutamate synthesis and growth. J Biol Chem 286: 27706–27717. [PubMed: 21636575]

Saunders EC, Ng WW, Kloehn J, Chambers JM, Ng M, and McConville MJ (2014) Induction of a Stringent Metabolic Response in Intracellular Stages of *Leishmania mexicana* Leads to Increased Dependence on Mitochondrial Metabolism. PLoS Pathog 10: e1003888. [PubMed: 24465208]

Sernee MF, Ralton JE, Dinev Z, Khairallah GN, O'Hair RA, Williams SJ, and McConville MJ (2006) *Leishmania* beta-1,2-mannan is assembled on a mannose-cyclic phosphate primer. Proc Natl Acad Sci U S A 103: 9458–9463. [PubMed: 16766650]

Vince JE, Tull D, Landfear S, McConville MJ (2011) Lysosomal degradation of *Leishmania* hexose and inositol transporters is regulated in a stage-, nutrient- and ubiquitin-dependent manner. Int. J. Parasitol 41, 791–800 [PubMed: 21447343]

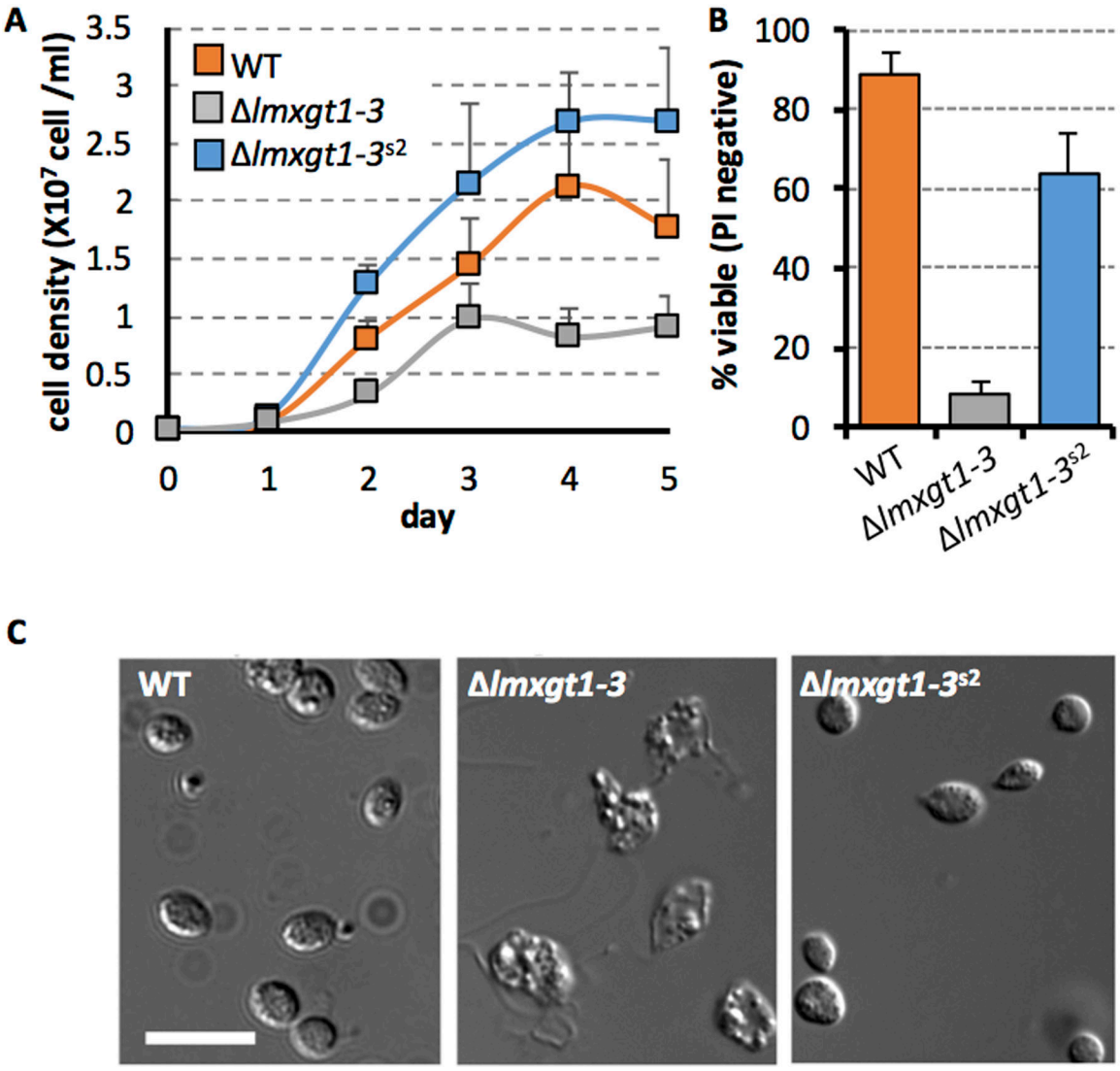

Figure 1. Isolation of the Δ*lmxgt1–3*^{s2} suppressor line with partially restored growth in rich medium and capacity to differentiate to amastigotes

A. Wild type, Δ*lmxgt1–3* and *Δlmxgt1–3*^{s2} promastigotes were cultivated in RPMI medium supplemented with 10% iFCS and change in cell density monitored over 5 days (representative experiment, average +/− standard deviation).

B. Stationary phase wild type, Δ*lmxgt1–3* and *Δlmxgt1–3*^{s2} promastigotes were induced to differentiate to amastigotes following transfer to RPMI medium containing 20 % iFCS, pH 5.5 at 33°C. Parasite viability was assessed by propidium iodide staining after 48 hours (n= 3x).

C. DIC microscopy of wild type, Δ*lmxgt1–3* and *Δlmxgt1–3*^{s2} promastigotes 5 days after induction of amastigote differentiation. Scale bar 10 μm.

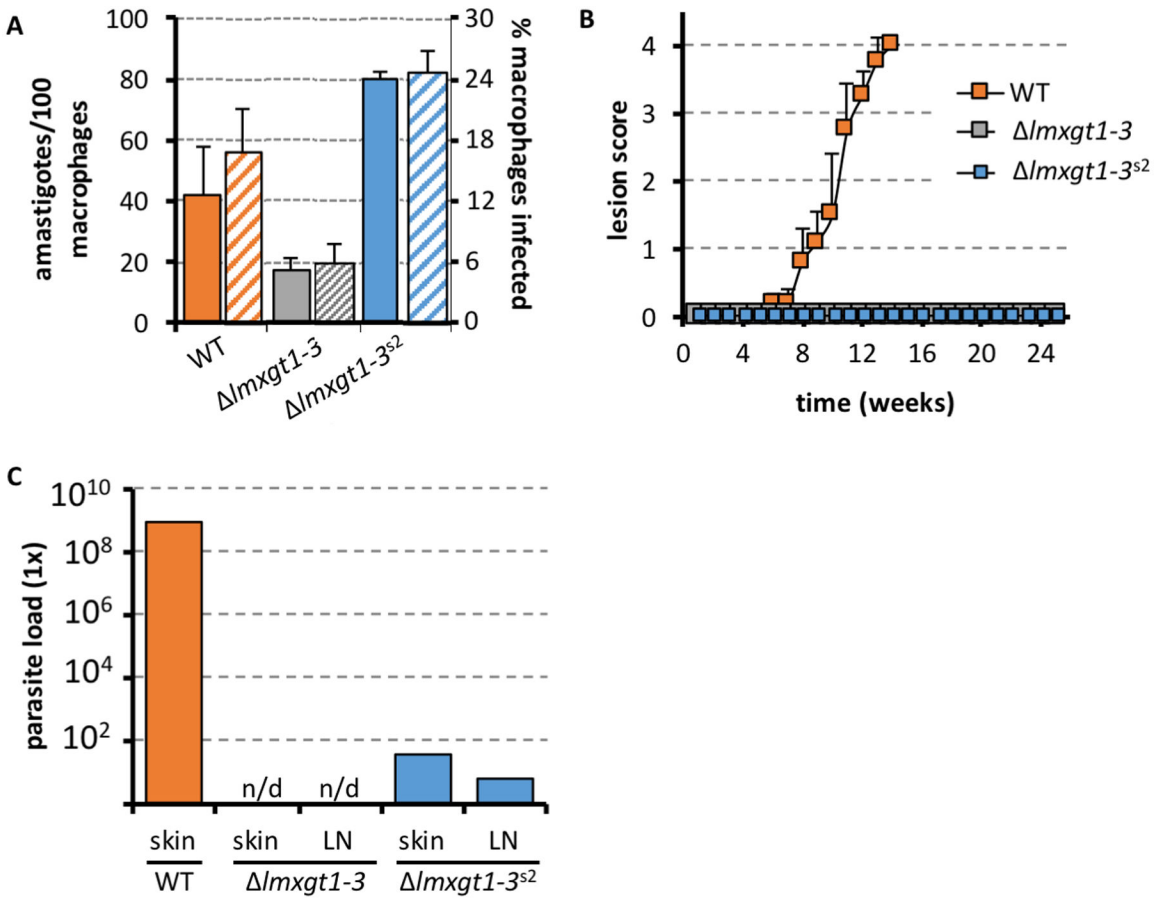

Figure 2. Infectivity of Δ*lmxgt1–3*^{s2} parasites in macrophages and in animal models

A. RAW macrophages were infected with stationary phase wild type, Δ*lmxgt1–3* and *Δlmxgt1–3*^{s2} promastigotes for 4 hours (MOI 10:1). Infected macrophages were washed to remove non-internalized parasites, and cultured at 34 °C (5 % CO_2) for 5 days and parasite numbers measured by microscopy. Parasite burden is expressed as number of amastigotes/100 macrophages' (solid fill) and percent macrophages infected (striped fill). The mean and standard deviation of 3 independent replicates (with >100 macrophages counted per replicate) are presented.

B. BALB/c mice were infected with wild type, Δ*lmxgt1–3* and *Δlmxgt1–3*^{s2} promastigotes (2×10^6 parasites in stationary growth phase). Lesion size was measured weekly.

C. Tissue samples from the site of infection (skin) and lymph nodes (LN) from infected mice culled at 15 weeks were serially diluted (1/10) in RPMI medium containing 10% iFCS. Parasite load was based on highest dilution that gave viable parasites after cultivation for 10 days at 27 °C. n/d; not detected,

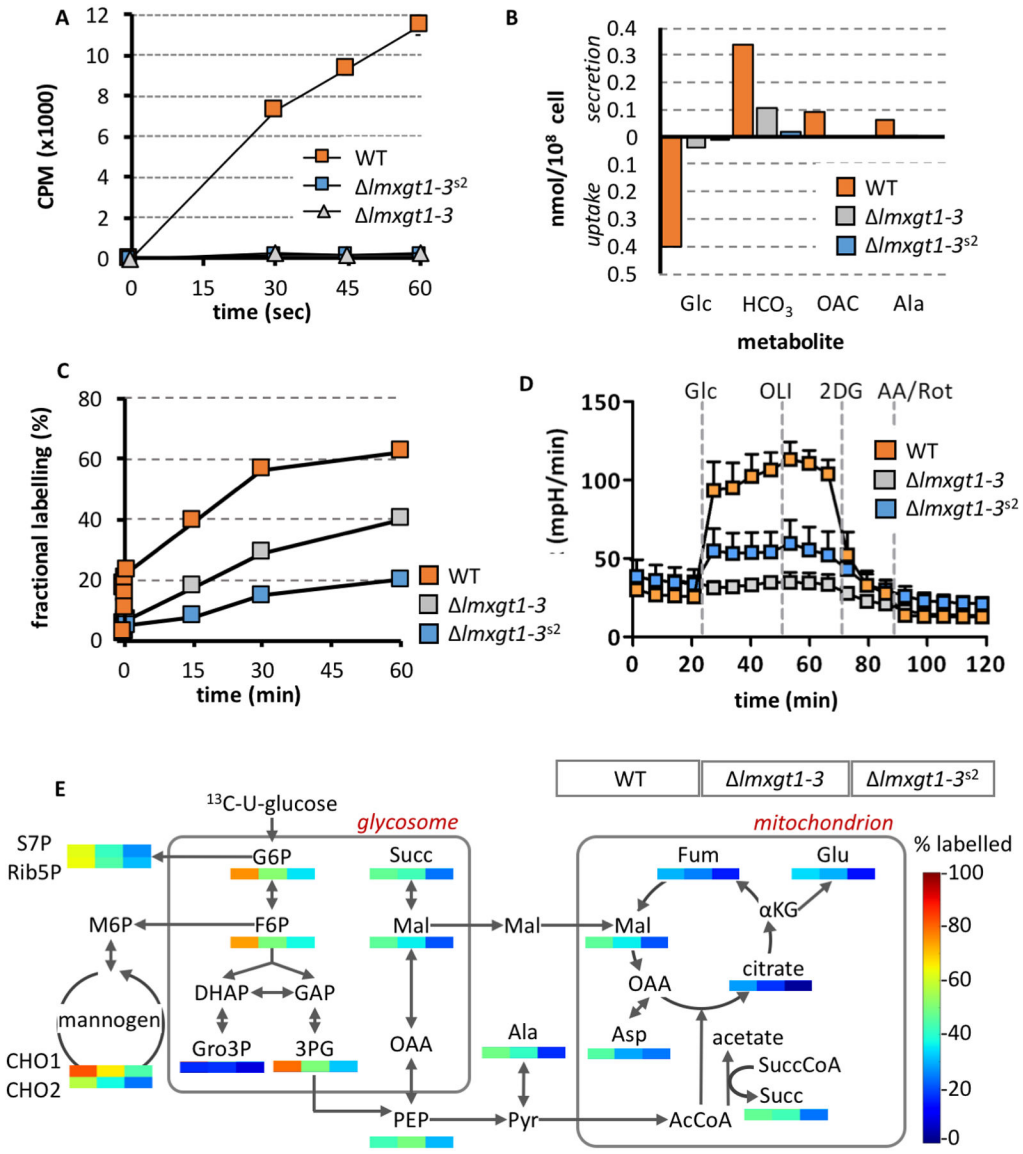

Figure 3. Δ*lmxgt1–3*^{s2} parasites exhibit reduced rates of glucose catabolism compared to wild type and parental Δ*lmxgt1–3* parasites.

A. Wild type, Δ*lmxgt1–3* and *Δlmxgt1–3*^{s2} promastigotes were suspended in RPMI containing ^{14}C-glucose (1 mM) and rapidly centrifuged through an aqueous/oil interface at indicated time points. Uptake was determined by liquid scintillation counting of ^{14}C-label in the cell pellet. Results are presented as mean and standard deviation of triplicate analyses.

B. Wild type, Δ*lmxgt1–3* and *Δlmxgt1–3*^{s2} promastigotes were suspended in completely defined medium (CDM) containing 0.5 mM ^{13}C-U-glucose for 24 hours. Rates of ^{13}C-glucose (Glc) utilization and secretion of ^{13}C-labeled end-products (bicarbonate, HCO_3; acetate, OAC; and alanine, Ala) was determined by ^{13}C NMR analysis of the medium after 24 hours.

C. Wild type, Δ*lmxgt1–3* and *Δlmxgt1–3*^{s2} promastigotes were cultivated in CDM containing ^{13}C-U-glucose (1 mM) and changes in ^{13}C-enrichment in glucose-6-phosphate determined by GC-MS.

D. Rates of glycolysis for wild type, Δ*lmxgt1–3* and *Δlmxgt1–3*^{s2} promastigotes was determined using the Seahorse metabolic analyzer following addition of glucose (Glc), oligomycin (OLI; inhibitor of mitochondrial ATP synthase), 2-deoxyglucose (2DG, inhibitor of glycolysis) and antimycin A/rotenone (AA/Rot, inhibitors of mitochondrial respiratory chain)

E. Wild type, Δ*lmxgt1–3* and *Δlmxgt1–3*^{s2} promastigotes were metabolically labeled with ^{13}C-U-glucose for 3 hours in CDM and fractional labeling determined for 33 intermediates in central carbon metabolism by GC-MS. Abbreviations used are as follows; G6P, glucose 6-phosphate; F6P, fructose 6-phosphate; S7P, seduheptulose 7-phosphate; Rib5P, ribulose 5-phosphate; M6P, mannnose-6-phosphate; 3PG, 3-phosphoglyceric acid; Gro3P, glycerol 3-phosphate; PEP, phosphoenolpyruvate; Succ, succinate; Mal, malate; Fum, fumarate; Cit, citrate; Ala, alanine; Asp, aspartate; αKG, α-ketoglutarate; Glu, glutamate.

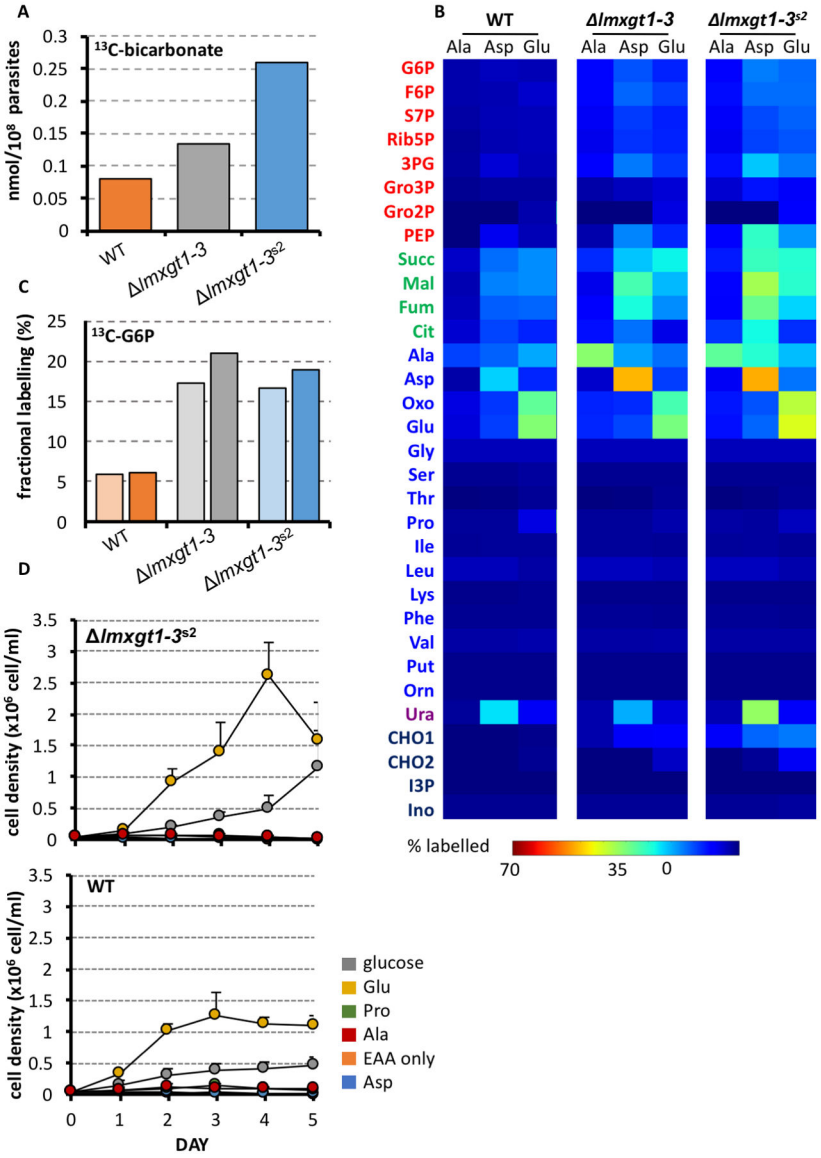

Figure 4. Δ*lmxgt1–3*^{s2} promastigote stages utilize NEAA as alternative carbon sources.

A. Wild type, Δ*lmxgt1–3* and *Δlmxgt1–3*^{s2} promastigotes were metabolically labeled with a mixture of ^{13}C-U-amino acids and the rate of mitochondrial respiration determined by measuring production of $^{13}CO_2$ (detected as $H^{13}CO_3$) by ^{13}C-NMR of the culture supernatant.

B. Wild type, Δ*lmxgt1–3* and *Δlmxgt1–3*^{s2} promastigotes were metabolically labeled with individual ^{13}C-NEAA (Ala, Asp, Glu). Parasite metabolism was quenched after 3 hours and ^{13}C-enrichment in selected carbon cycle intermediates determined by GC-MS.

Abbreviations as in Figure 3 legend and Gro2P, glycerol 2-phosphate; Oxo, oxo-proline; Gly, glycine; Ser, serine, Thr, threonine; Pro, proline; Ile, isoleucine; Leu, leucine; Lys, lysine; Phe, phenylalanine; Val, valine; Put, putrescine; Orn, ornithine; Ura, uracil; CHO1, carbohydrate 1; CHO2, carbohydrate 2; I3P, inositol 3-phosphate; Ino, myo-inositol.

C. Wild type, Δ*lmxgt1–3* and *Δlmxgt1–3*^{s2} promastigotes were metabolically labeled with ^{13}C-U-glycerol for 30 min (light orange/grey/blue) or 60 min (dark orange/grey/blue) and the rate of gluconeogenesis determined from fractional labeling of glucose-6-phosphate (G6P).

D. Wild type or *Δlmxgt1–3*^{s2} promastigotes were cultivated in Glc^{-}/NEAA^{-}-CDM with or without supplementation with specific NEAA (6 mM) or glucose (6 mM) (n=3, mean +/− SEM).

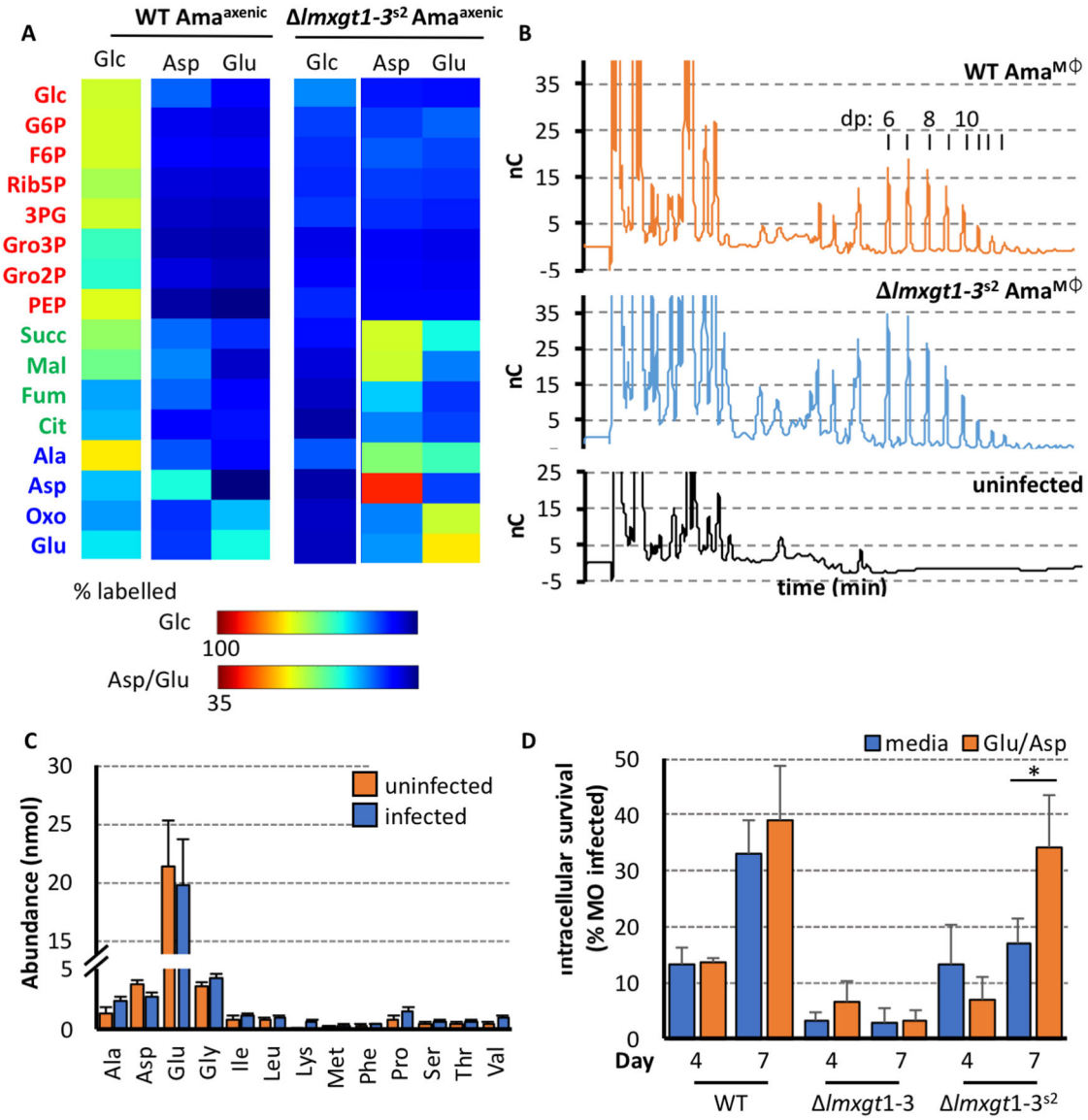

Figure 5. Δ*lmxgt1–3*^{s2} amastigotes metabolise a range of alternative carbons sources via a functional TCA cycle

A. Wild type and *Δlmxgt1–3*^{s2} Ama^{axenic} were labeled with ^{13}C-U-glucose, ^{13}C-U-aspartate or ^{13}C-U-glutamate for 3 hours and ^{13}C-enrichment (presented as fractional labelling) of selected carbon cycle intermediates determined by GC-MS. Note different scales used for representing ^{13}C-enrichment in glucose versus amino acid labeling experiments.

B. Analysis of mannogen levels in intracellular wild type and *Δlmxgt1–3*^{s2} amastigotes. Mannogen was extracted from J774 macrophages that had been infected for 5 days with either wild type or *Δlmxgt1–3*^{s2} parasites. Mannogen oligomers (with degree of polymerization (dp) of 6 to >12 mannose residues) were detected by HPAEC with amperometric detection (nC, nanoCoulombs). Mannogen oligomers were not detected in uninfected J774 macrophages.

C. Bone marrow macrophages (2×10^6 cells total) were infected with WT *L. mexicana* promastigotes (MOI 5:1). The macrophages were maintained for 24 hours before metabolism was quenched and intracellular amino acid pools quantified by GC-MS.
D. The culture media of bone marrow derived macrophages infected (MOI 5:1) with either wild type, *Δlmxgt1–3, or Δlmxgt1–3*^{s2} promastigotes was supplemented with an additional 6 mM aspartate or glutamate. Intracellular survival (expressed as percent infected macrophage) determined after 4 and 7 days (n=3, 100 macrophages counted per replicate; average, mean +/− standard deviation; * p-value<0.05)

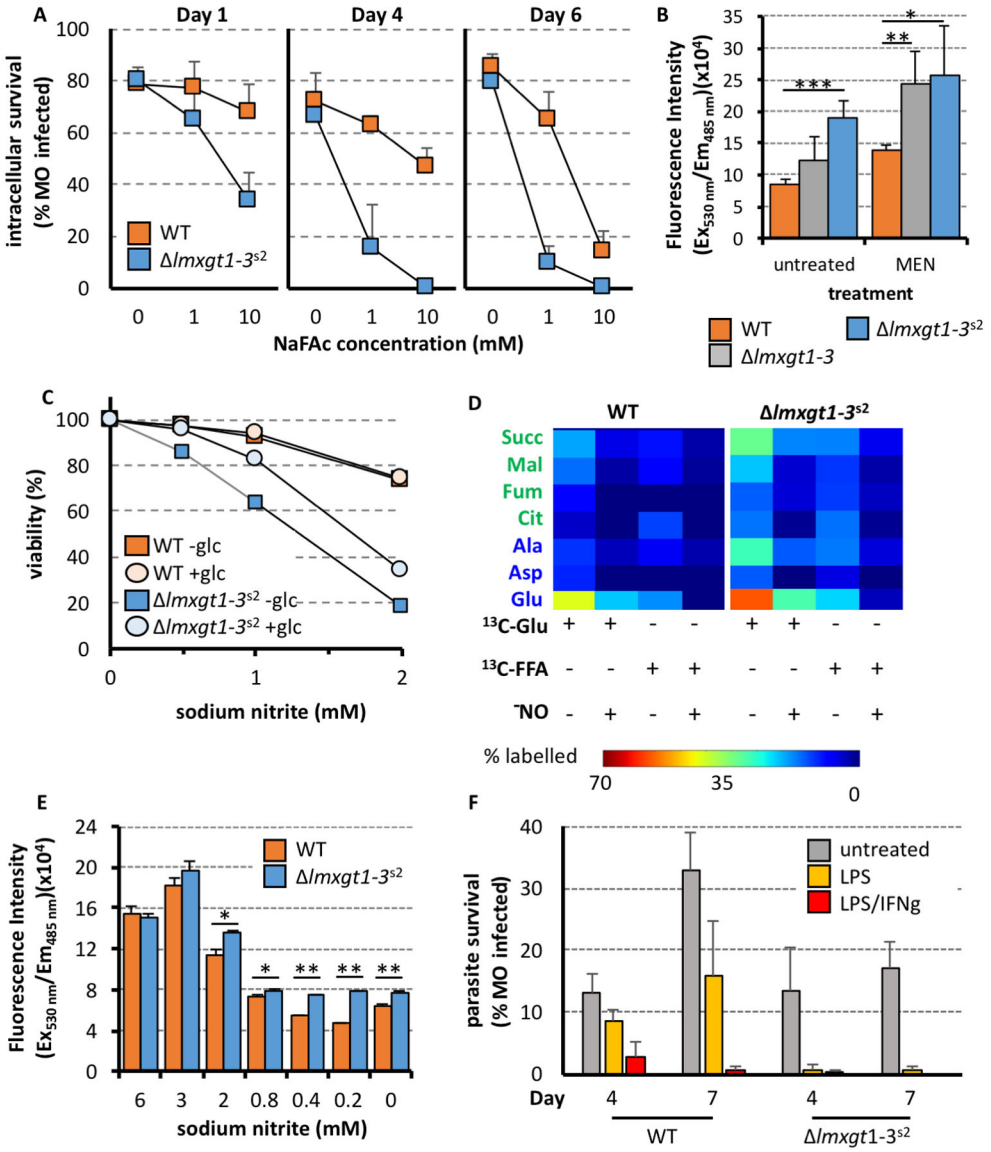

Figure 6. Δ*lmxgt1–3*^{s2} amastigotes are dependent on a functional TCA cycle and susceptible to nitric oxide.

A. Bone marrow derived macrophages infected (MOI 5:1) with either wild type or *Δlmxgt1–3*^{s2} amastigotes, were treated with 0, 1 or 10 mg/ml sodium fluoroacetate (NaFAc) and intracellular survival, expressed as percent infected macrophage, determined after 1, 4 and 6 days (representative experiment; n=4, 100 macrophages counted per replicate, average +/− standard deviation).

B. Levels of reactive oxygen species (ROS) in wild type, Δ*lmxgt1–3* and *Δlmxgt1–3*^{s2} promastigotes. Promastigotes were suspended in glucose-free RPMI supplemented with 10 % iFCS for 2.5 hours at 27 °C prior to the addition of 2.5 μM menadione (MEN) to increase mitochondrial metabolism or mitochondrial ROS production, respectively. Parasites were labeled with H2DCFDA (30 min, 27 °C) to detect ROS and fluorescence normalised to unlabeled parasites (representative experiment; n=3; average, +/− standard deviation; * p-value<0.07, ** p-value <0.05, *** p-value <0.005).

C. Wild type and *Δlmxgt1–3*^{s2} Ama^{axenic} were suspended in glucose-free RPMI with 20% iFCS (pH 4.5) containing 0–2 mM sodium nitrite with or without glucose supplementation, and incubated at 35 °C overnight. Amastigote viability was determined after eFluor staining and FACS analysis and normalization to untreated controls.

D. Wild type and *Δlmxgt1–3*^{s2} Ama^{axenic} were cultured in CDM containing 1 mM sodium nitrite and either ^{13}C-U-glutamate or mixed ^{13}C-U-free fatty acids. Parasite metabolism was quenched after 3 hours and the ^{13}C-enrichment (presented as fractional labelling) of selected carbon cycle intermediates was determined by GC-MS.

E. Wild type and *Δlmxgt1–3*^{s2} Ama^{axenic} were cultured in RPMI supplemented with 20 % iFCS (pH 4.5) containing varying concentrations of sodium nitrite (0 to 6 mM) for 2 hours. Parasites were labeled with H2DCFDA (30 min, 33–34 °C) to detect ROS and fluorescence normalized to unlabeled parasites (representative experiment; n=3; average, +/− standard deviation; * p-value<0.005, ** p-value <0.0005).

F. Bone marrow derived macrophages infected (MOI 5:1) with either wild type, *Δlmxgt1-*^{2} or *Δlmxgt1–3*^{s2} promastigotes, were stimulated with lipopolysaccharide (LPS 20 ng/ml) or LPS and interferon gamma (LPS/IFNγ, 20 and 10 ng/ml, respectively) and intracellular survival (expressed as percent infected macrophage) determined after 4 and 7 days (representative experiment; n=3, 100 macrophages counted per replicate; average, +/− standard deviation).

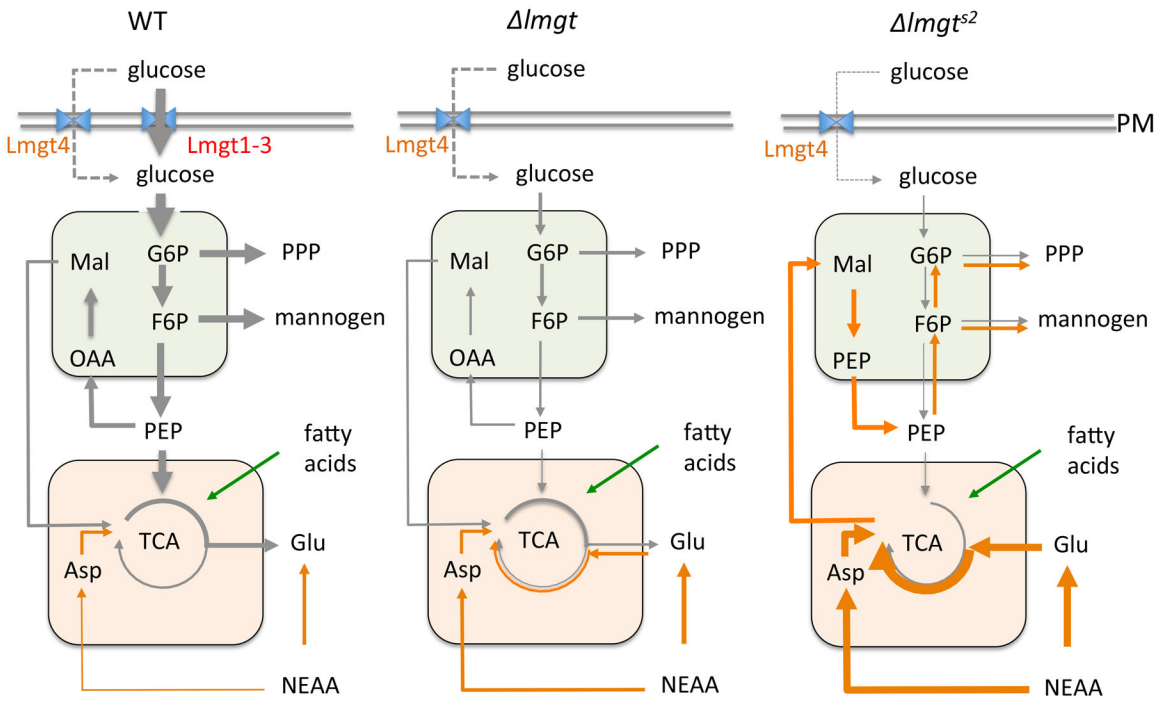

Fig 7. Schematic summary of central carbon metabolism of wild type, Δ*lmxgt1–3* and Δ*lmxgt1–3*^{s2} amastigotes.

The Δ*lmxgt1–3* mutant line partially adapts to loss of LmxGT1–3 by increasing expression of the plasma membrane transporter, LmxGT4, as well as increased uptake of NEAA. The *Δlmxgt1–3*^{s2} line exhibits a more robust adaptation to glucose deprivation with increased metabolism of NEAA (particularly glutamate) in the mitochondria (orange compartment) and gluconeogenesis in glycosomes (green compartment)